



# AMERICAN METEOROLOGICAL SOCIETY

*Bulletin of the American Meteorological Society*

## **EARLY ONLINE RELEASE**

This is a preliminary PDF of the author-produced manuscript that has been peer-reviewed and accepted for publication. Since it is being posted so soon after acceptance, it has not yet been copyedited, formatted, or processed by AMS Publications. This preliminary version of the manuscript may be downloaded, distributed, and cited, but please be aware that there will be visual differences and possibly some content differences between this version and the final published version.

The DOI for this manuscript is doi: [10.1175/BAMS-D-13-00203.1](https://doi.org/10.1175/BAMS-D-13-00203.1)

The final published version of this manuscript will replace the preliminary version at the above DOI once it is available.



# A Long-Term, High-quality, High Vertical Resolution GPS Dropsonde Dataset for Hurricane and Other Studies

Junhong (June) Wang<sup>1,2</sup>, Kate Young<sup>1</sup>, Terry Hock<sup>1</sup>, Dean Lauritsen<sup>1</sup>, Dalton Behringer<sup>1</sup>,  
Michael Black<sup>3</sup>, Peter G. Black<sup>4</sup>, James Franklin<sup>5</sup>, Jeff Halverson<sup>6</sup>, John Molinari<sup>2</sup>, Leon  
Nguyen<sup>2</sup>, Tony Reale<sup>7</sup>, Jeff Smith<sup>8</sup>, Bomin Sun<sup>9</sup>, Qing Wang<sup>10</sup>, Jun A. Zhang<sup>3,11</sup>

1. National Center for Atmospheric Research\*, Boulder, CO, USA
2. DAES, University at Albany, SUNY, Albany, NY
3. NOAA/HRD, Miami, FL
4. Science Applications International Corporation, Inc., Monterey, CA
5. NOAA/NHC, Miami, FL
6. University of Maryland Baltimore County, Baltimore, MD
7. NOAA/NESDIS, Camp Springs, MD
8. NOAA/AOC, Macdill AFB, FL
9. I.M. Systems Group, Rockville, MD
10. NPS, Monterey, CA
11. RSMAS, University of Miami, Miami, FL

Bulletin of American Meteorological Society

Revised on August 20, 2014

*Corresponding Author:*

Junhong (June) Wang

Department of Atmospheric & Environmental Sciences

University at Albany, SUNY

1400 Washington Ave., Albany, NY 12222

Phone: (518) 442-3478; Email: junhong@ucar.edu

---

\* The National Center for Atmospheric Research is sponsored by National Science Foundation.

29 **Capsule**

30

31 A long-term (1996-2012), high-quality, high vertical resolution (~5-15 m) GPS dropsonde  
32 dataset is created from NOAA Hurricane flights and consists of 13,681 atmospheric profiles for  
33 120 tropical cyclones.

34

35

36 **Abstract**

37

38 A GPS dropsonde is a scientific instrument deployed from research and operational aircraft that  
39 descends through the atmosphere by a parachute. The dropsonde provides high-quality, high  
40 vertical resolution profiles of atmospheric pressure, temperature, relative humidity, wind speed  
41 and direction from the aircraft flight level to the surface over oceans and remote areas. Since  
42 1996, GPS dropsondes have been routinely dropped during hurricane reconnaissance and  
43 surveillance flights to help predict hurricane track and intensity. From 1996 to 2012, NOAA has  
44 dropped 13,681 dropsondes inside hurricane eye walls or in the surrounding environment for 120  
45 tropical cyclones (TCs). All NOAA dropsonde data have been collected, reformatted to one  
46 format, and consistently and carefully quality-controlled using state-of-art quality-control (QC)  
47 tools. Three value-added products, the vertical air velocity and the radius and azimuth angle of  
48 each dropsonde location, are generated and added to the dataset. As a result, a long-term (1996-  
49 2012), high-quality, high-vertical resolution (~5-15 m) GPS dropsonde dataset is created and  
50 made readily available for public access. The dropsonde data collected during hurricane  
51 reconnaissance and surveillance flights have improved TC track and intensity forecasts  
52 significantly. The milestones of dropsonde data's impact on hurricane studies are summarized.  
53 The scientific applications of this long-term dropsonde dataset are highlighted, including  
54 characterizing TC structures, studying TC environmental interactions, identifying surface-based  
55 ducts in hurricane environment which affect electromagnetic wave propagation, and validating  
56 satellite temperature and humidity profiling products.

57 **1. Introduction**

58

59 An hurricane is one of the most devastating extreme weather phenomena threatening the  
60 United States. In the US, between 1980-2012 over \$1 trillion were spent providing disaster relief  
61 aid after 151 weather disasters, each of which overall damages and costs reached or exceeded \$1  
62 billion (Source <http://www.ncdc.noaa.gov/billions/>). Of those 151 events, 33 of the disasters  
63 resulted from tropical cyclones and they accounted for ~50% of the total damage in dollars.  
64 Early warning, adequate preparation time and evacuation time rely on accurate forecasting of  
65 hurricane tracks and intensities, and these forecasts depend on accurate measurements of  
66 hurricane winds and thermodynamic structure.

67 A dropsonde is a scientific instrument dropped from research aircraft or other platforms in  
68 the air and descends through the atmosphere by a parachute to make measurements of pressure,  
69 temperature, relative humidity (RH), and horizontal wind speed and direction profiles at any  
70 location over the globe, especially over ocean or remote regions where other in-situ  
71 measurements are hard to make. NCAR's GPS Dropsonde System known as AVAPS (Airborne  
72 Vertical Atmospheric Profiling System) was developed in the 1990s and is the only operational  
73 dropsonde system in the world capable of providing research-quality, high-resolution, reliable  
74 atmospheric profiles in hard-to-reach locations. This system consists of on-board data acquisition  
75 and processing system and the dropsonde itself. The GPS dropsonde is currently manufactured  
76 by Vaisala, Inc., under license from NCAR, and is also known as Vaisala dropsonde RD94  
77 (Hock and Franklin 1999; Vaisala 2014). The dropsonde includes a pressure, temperature,  
78 humidity sensor module (referred as PTU sensor module hereafter), a GPS receiver for wind  
79 measurements, and a 400-MHz telemetry transmitter to transmit data from the sonde to the

80 onboard receiving system (see Fig. 1 in Hock and Franklin 1999). Based on Vaisala (2014), the  
81 accuracy of pressure, temperature and RH is 0.4 hPa, 0.2°C and 2%, respectively. The horizontal  
82 wind measurement from u-blox GPS receiver is estimated to be 0.1 m/s. The aircraft data system  
83 includes a narrowband 400-MHz telemetry receiver, which allows simultaneous operation of up  
84 to eight dropsondes in the air. During last 18 years (1996-2013), the dropsonde system has  
85 improved significantly, including a complete redesign of the system (known as AVAPS II) in  
86 2008 and development of miniaturized dropsondes for deployment from super-pressure balloons,  
87 unmanned aerial vehicles (UAVs) and high-altitude aircraft during recent years. Major  
88 milestones in AVAPS advancement and scientific impact during its lifetime are summarized in  
89 Table 1.

90 Since 1996, GPS dropsondes have been routinely deployed during hurricane reconnaissance  
91 and surveillance flights to help predict hurricane tracks and intensities. The reconnaissance  
92 flights are conducted in the hurricane inner and outer core region, while the surveillance aircraft  
93 fly outside of the immediate environment of tropical cyclones. During the first season of NOAA  
94 Gulfstream-IV (G-IV) jet aircraft missions for hurricanes in 1997, about 150 dropsondes were  
95 released from the aircraft at 150-200 km intervals in the environment of TCs (Aberson and  
96 Franklin 1999). This first set of dropsonde observations improved mean hurricane track forecasts  
97 from the Geophysical Fluid Dynamics Laboratory hurricane model by as much as 32% and  
98 intensity forecasts by 20% during the critical first two days of the forecast (Aberson and Franklin  
99 1999). The track forecast improvements were comparable to those accumulated over the past 20-  
100 25 years at that time (Aberson and Franklin 1999). Mean track forecast improvement as a result  
101 of synoptic surveillance dropsondes during 1999-2005 is summarized in Fig. 1. The  
102 improvement is all above 10% during 0-48 hours in the Global Forecast System (GFS) model

103 (Fig. 1). This result is consistent with the finding in Abernson (2010). The dropsonde data have  
104 also been found to play an important role in understanding the characteristics of hurricane  
105 dynamic and thermodynamic structures (e.g., Franklin et al. 2003; Molinari et al. 2012; Zhang et  
106 al. 2013). For example, Franklin et al. (2003) analyzed 630 dropsonde profiles from hurricane  
107 reconnaissance flights during the 1997-1999 seasons and documented, for the first time, the  
108 mean vertical profile of wind speed in the hurricane inner core from the surface to the 700-hPa  
109 level with unprecedented accuracy and resolution. In addition to routine hurricane flights, the  
110 dropsonde is also often deployed to study winter storms, TCs in different ocean basins, strong  
111 convection systems and other severe weather events to ultimately improve their forecasting. A  
112 study of dropsonde impact during the 1999 NOAA winter storm reconnaissance (WSR) program  
113 documented that the dropsonde data significantly improved the forecasts in 18 of the 25 storms  
114 targeted by NOAA aircraft (Szunyogh et al. 2000). However, the WSR program has been  
115 cancelled recently due to minimal impact in recent years, perhaps due to other improvements in  
116 the data assimilation systems (Hamill et al. 2013). The impact of dropsonde data on typhoon  
117 track forecasts has been also studied extensively (e.g., Wu et al. 2007; Abernson 2011; Chou et al.  
118 2011; Wu et al. 2012). For example, the typhoon track forecast error in four numerical weather  
119 prediction models was reduced by 20-40% consistently as a result of dropsonde data collected  
120 during T-PARC (The Observing System Research and Predictability Experiment (THORPEX)  
121 Pacific Asian Regional Campaign experiment) in 2008 (Weissmann et al. 2011).

122 In spite of the scientific importance of the dropsonde data collected from all of these  
123 missions and projects mentioned above, the data reside in different locations, have different  
124 formats and varied levels of data quality, and in many cases have limited metadata. Such

125 heterogeneity between datasets hinders composite analysis of TCs and limits the application of  
126 the dropsonde data for broader scientific use.

127

## 128 **2. Data Sources, Quality Assurance and Control and Value-Added Products**

129

130 Raw dropsonde data for this study were collected during NOAA hurricane reconnaissance  
131 and surveillance flights from 1996 to 2012 and were obtained from NOAA's Hurricane Research  
132 Division (HRD) Online GPS-Dropsonde Data Archive

133 ([http://www.aoml.noaa.gov/hrd/Storm\\_pages/sondeformat.html](http://www.aoml.noaa.gov/hrd/Storm_pages/sondeformat.html)). The NOAA Aircraft  
134 Operations Center (AOC) runs the AVAPS program for NOAA. The dropsonde data available  
135 through the NOAA HRD site were collected by HRD, National Hurricane Center (NHC), and the  
136 Air Force (USAF), three of the biggest users of the AVAPS dropsonde system. The dropsonde  
137 data contained in this archive were collected from three separate aircraft. The NOAA N42RF and  
138 N43RF are P3 aircraft and the NOAA N49RF is a G-IV. The P3 aircraft make measurements  
139 from the inner and outer core (0 to about 200 km radius) and from the middle-lower troposphere  
140 (1-5 km) to the surface. The atmospheric data outside of the immediate environment of TCs  
141 come primarily from the NOAA G-IV flying at ~14-15 km altitude. Note that during 1996-2012  
142 about 6000 soundings were collected from USAF, but they are not processed and included in this  
143 archive.

144 The data quality assurance (QA) begins with the cumbersome task of renaming all of the  
145 sounding files according to date and time of launch. The files were originally archived only by  
146 sonde ID number. The next step is to identify and categorize the files according to dropsonde  
147 GPS type (u-blox or GPS121). This is necessary because a new dropsonde with an improved full



148 GPS receiver (u-blox), capable of making more accurate measurements of position and velocity,  
149 was introduced in 2005. Prior to that, GPS121 dropsondes were used. The GPS121 receiver  
150 computed the 3-D velocity. But the 3-D position was computed using precise drop location from  
151 the AVAPS aircraft data system and integrating the velocity to obtain position with each  
152 individual measurement from the dropsonde. From 2005 through 2007 both sonde types were  
153 deployed by different aircraft in different storms. The implication of having varying dropsonde  
154 types is that quality control of the GPS data must be handled differently. Finally, before data  
155 quality control could begin, the data files were categorized according to the aircraft they were  
156 collected from.

157 Data quality control of the sounding data is an extensive, multi-step process that includes  
158 evaluating the data products using a variety of visualization tools and statistical methods to  
159 identify and correct data quality issues caused by launch detect errors, sensor offsets or bias,  
160 accelerated descent rates, and failure of the sensors to accurately transmit data from flight level  
161 altitude to the ocean's surface. Each raw sounding data profile must be individually evaluated to  
162 determine if the data contain any features that warrant further investigation. Appropriate  
163 corrections are then applied. Metadata files are created for each aircraft flown in each of the  
164 storms and include documentation detailing specific data quality issues found in individual data  
165 files, and explains subsequent corrections, if any are applied. The variables, pressure,  
166 temperature, and RH, are calibrated values from measurements made by the dropsonde, all of  
167 which are subjected to quality control. The dew point is calculated from the quality controlled  
168 RH and temperature. The geopotential altitude is calculated from the hydrostatic equation,  
169 typically from the ocean's surface upward. Dropsondes that fail to transmit useful data to the  
170 surface must be identified so that geopotential altitude can be integrated from flight level down.

171 The descent rate of the sonde is computed using the time-differentiated hydrostatic equation.  
172 Wind speed and direction are quality controlled, but the GPS horizontal position (latitude and  
173 longitude) is not. Following evaluation of the raw data and subsequent steps to resolve data  
174 quality issues, each of the dropsonde profiles is processed through the Earth Observing  
175 Laboratory's Atmospheric Sounding Processing Environment (ASPEN) software, which further  
176 analyzes data quality and performs smoothing and filtering to remove suspect data points. The  
177 ASPEN configuration used to process this dataset is given in the dataset readme file. Following  
178 ASPEN, histograms of all variables are evaluated to examine the distribution, range, and  
179 characteristics of each parameter. Profile plots of the quality controlled soundings are visually  
180 evaluated for outliers, or any other obvious issues, and time-series plots are used to evaluate the  
181 consistency of soundings launched during each flight, and to examine the variability of  
182 soundings from different missions. These standard procedures are used to ensure the highest-  
183 quality set of soundings within and near a large and varied sample of TCs are provided to the  
184 community. In addition to pressure, temperature, humidity and wind speed and direction profiles,  
185 three value-added profiles, the vertical air velocity and the radius and azimuth angle of each  
186 dropsonde location, are computed as described in detail below and added to the dataset.

187 The vertical air velocity is computed as the difference between the actual dropsonde fall rate  
188 and that in the still air (Wang et al. 2009). The still-air fall rate is computed based on the balance  
189 between the gravity and the drag force, and it is a function of the weight of the dropsonde, the  
190 drag coefficient (0.61 for dropsonde) and the area of the parachute (Hock and Franklin 1999;  
191 Wang et al. 2009). The sonde weight of 350 g and 322 g is used for AVAPS-I or AVAPS-II  
192 sondes, respectively. A square parachute of 26 cm X 26 cm is used. A 20-s low-pass filter is  
193 applied to the calculated vertical velocity to remove occasional spikes. Both directly-calculated

194 and filtered velocities are saved in the data. The uncertainty in the vertical air velocity is  
195 estimated to be on the order of 1 m/s, and the velocities with magnitudes less than 1 m/s should  
196 not be used without careful examination (Wang et al. 2009).

197 For each sonde the radius of the observation was determined by the spherical distance from  
198 the storm center to the sonde location. Azimuth was determined trigonometrically from the  
199 latitudes and longitudes of the storm center and the sonde. The effects of lateral motion of the  
200 sonde were included, so that the radius and azimuth varied with height for each sonde. The storm  
201 center was defined by the six-hourly NHC Best Track position linearly interpolated to one-  
202 minute resolution. In reality the storms do not move linearly. Rather, the purpose of the high  
203 time resolution was to prevent artificial jumps in center position, and thus in sonde position, on  
204 small time scales.

205 The final quality-controlled dropsonde dataset includes 13,681 dropsonde soundings from  
206 1996 to 2012 for 120 storms. The numbers of soundings and storms for each year are shown in  
207 Fig. 2. There were maximum numbers of soundings (2,306) and storms (13) in 2005 (Fig. 2).  
208 The record number of soundings per storm (653) was deployed in Hurricane Ivan (2004). The  
209 majority of soundings were dropped over the Atlantic Ocean (Fig. 3). The sondes were dropped  
210 either from NOAA P3 aircraft in the inner or outer core regions from the middle to lower  
211 troposphere or NOAA G-IV in the surrounding regions from the upper troposphere (Fig. 3). Fig.  
212 4 shows one example of sonde locations dropped between 17 UTC and 24 UTC on August 28,  
213 2005 from NOAA P3 and G-IV aircraft for Hurricane Katrina. The number of dropsondes in  
214 each 100-km radial bin and each 30° azimuthal bin is displayed in Fig. 5. The dropsondes were  
215 most frequently located within 100 km to the tropical cyclone center (Fig. 5), and the number of  
216 dropsondes gradually decreased with increasing radius. The broad radial distribution of

217 dropsondes has enabled composite studies to be done on various spatial scales ranging from the  
218 TC inner core (Zhang et al. 2013) to the outer regions of the TC and the environment (Molinari  
219 et al. 2012). The azimuth distribution of dropsondes is rather asymmetric, with a maximum in  
220 the northern quadrant and a minimum in the southern quadrant (Fig. 5).

221 The QCed dropsonde data include high-quality and high vertical resolution profiles of  
222 pressure, temperature, RH, wind speed and direction, vertical velocity, sonde location (longitude,  
223 latitude, altitude), and radius and azimuth angle relative to the storm centers. The  
224 thermodynamical and wind data are available at half-second and quarter-second resolution,  
225 respectively, corresponding to ~5-15 m and ~3-8 m from the surface to 16 km altitude. The final  
226 dropsonde dataset is in EOL sounding file format that includes a header, with detailed project  
227 and sounding information, and seventeen columns of high resolution data. The EOL format is an  
228 ASCII text format and is described in details in the readme file on the dataset website. The files  
229 are broken out into directories by year, storm name, GPS sensor type, and aircraft type. The  
230 dataset along with the readme file is available for free download on  
231 <https://www.eol.ucar.edu/content/noaa-hurricane-dropsonde-archive>.

232

### 233 3. Scientific Highlights

234

235 Dropsonde data have been used extensively for hurricane and other studies. In the  
236 introduction, we summarized milestones of dropsonde data's impact on hurricane studies.  
237 Several scientific applications of this long-term dropsonde dataset are highlighted below based  
238 on preliminary analysis of the data. They not only demonstrate the scientific value of this dataset  
239 but also illustrate potential scientific discovery in the future as a result of this dataset.

240 Composite profiles of GPS-derived wind measurements in TCs in the Atlantic Basin were  
241 constructed from 3,101 dropsonde profiles from this dataset (Fig. 6). Selection criteria consisted  
242 of all drops from NOAA P3 aircraft only. A large fraction of the dropsondes from P3 aircraft  
243 were dropped into storms that were not hurricane status, or storms that changed categories during  
244 the process of dropping, so they were excluded in this analysis. Only storms that maintained their  
245 status through the entire drop (e.g., didn't fluctuate in intensity) were used. If there was any  
246 question of ambiguity in intensity, the sondes were not included. Mean profiles of wind speed  
247 stratified according to hurricane intensity are shown in Figure 6. Composites were constructed by  
248 averaging individual profiles with a rough mean vertical bin resolution of 25 m, and we applied a  
249 conservative smoothing routine to reduce the profile noise. The total sample encompasses data  
250 for 667 Category One, 710 Category Two, 670 Category Three, 908 Category Four and 146  
251 Category Five storms. No attempt was made to stratify drops according to radial distance within  
252 each intensity class. Regardless, these mean profiles show robust differences between the five  
253 hurricane intensity classes. All profiles reveal significant shear in the boundary layer and low-  
254 level wind maxima between 500-1000 m above ground. The difference in mean-profile wind  
255 speed between individual storm categories is remarkably linear, particularly with regard to the  
256 lower tropospheric wind maximum. In all categories, there is a tendency for wind speed to  
257 weaken significantly above 3-4 km. Interestingly, secondary maxima appear around 4 km in two  
258 of the stronger categories (Category Three and Four). It is uncertain whether absence of this  
259 feature in the Category Five wind profile is related to physical processes or a limited sample size.  
260 This type of composite-based analysis just scratches the surface of what can be done using this  
261 high-resolution, vertical structure information.

262 Dropsonde data have often been used to study changes in the TC structure in response to  
263 environmental vertical wind shear (e.g. Molinari et al. 2012; Zhang et al. 2013). Shear has been  
264 shown to have a negative influence on the TC intensity change (e.g., DeMaria et al. 2005)  
265 through several proposed mechanisms. One hypothesized mechanism is the thermodynamic  
266 modification of the inflow layer by downdrafts induced by asymmetric convection outside the  
267 inner core (Riemer et al. 2010; 2013). To assess this, the position of each dropsonde was rotated  
268 with respect to the environmental vertical wind shear following Corbosiero and Molinari (2002).  
269 The environmental shear was taken from the Statistical Hurricane Intensity Prediction Scheme  
270 (SHIPS) database (DeMaria et al. 2005). Figure 7 shows the mean equivalent potential  
271 temperature ( $\theta_e$ ) in each shear-relative quadrant in the 75-200 km radii region, which in general  
272 falls well outside the eye wall. Only sondes released when ambient shear exceeded  $6 \text{ m s}^{-1}$  are  
273 included. Note that the number of dropsondes reporting data decreased rapidly above 2-km  
274 height (Fig. 7). These results are compared to similar fields shown within the eyewall region by  
275 Zhang et al. (2013). In the lowest km for both studies,  $\theta_e$  reaches a minimum in the downshear-  
276 left quadrant and a maximum right of the shear vector. This likely reflects the influence of low-  
277  $\theta_e$  downdrafts left of shear and surface flux-induced boundary layer recovery right of shear  
278 (Molinari et al. 2013; Zhang et al. 2013). Fig. 7 shows that these anomalies extend up to 3 km  
279 elevation and out to 200 km from the center. Dropsondes can be divided up by a combination of  
280 radius, ambient shear magnitude, tropical cyclone intensity, and/or intensity change to further  
281 elucidate the role of vertical wind shear in TC structure.

282 The hurricane boundary layer (HBL) has long been known to play an important role in storm  
283 development and intensification (e.g., Emanuel 1986; Braun and Tao 2000; Smith et al. 2009;  
284 Bryan and Rotunno 2009). Understanding of the HBL structure becomes increasingly important

285 as efforts have been made toward developing high-resolution numerical models in order to  
286 improve the hurricane intensity forecast (e.g., Gopalakrishnan et al. 2013; Rogers et al. 2013).  
287 However, the HBL has been the least observed part of a storm until now, especially its  
288 turbulence structure (Black et al. 2007; Zhang et al. 2008; Zhang 2010). With the advent of the  
289 GPS dropsonde (Hock and Franklin 1999; Franklin et al. 2003), the mean boundary layer  
290 structure has been progressively studied, mostly the boundary layer structure in an individual  
291 storm (e.g., Bell and Montgomery 2008; Barnes 2008). Recent composite analyses of GPS  
292 dropsonde data (Zhang et al. 2011; 2013) from multiple hurricanes at various stages of their  
293 lifecycle have provided a more comprehensive representation of the HBL. In spite of those  
294 efforts using the dropsonde data to study the HBL, it still remains imperative to include more  
295 dropsonde soundings, such as those from this study, to understand the HBL processes and  
296 improve its representation in numerical models, and ultimately increase our ability to better  
297 forecast hurricane.

298 Vertical profiles of temperature and specific humidity are two key parameters that characterize  
299 the environmental conditions for electromagnetic (EM) wave propagation in the atmosphere,  
300 represented by the modified index of refraction,  $M$  (Bean and Dutton 1966). The data source for  
301 this purpose generally comes from numerical simulations and/or mostly by rawinsonde  
302 measurements based on ships, islands, or land. While rawinsondes provide direct measurements  
303 of the atmospheric temperature and moisture, it is generally difficult to use the measurements for  
304 identifying surface-based ducts or evaporative ducts over the ocean due to ship or island  
305 contaminations unless an up-down sampling approach is adopted. Although the sensor  
306 technology between dropsondes and rawinsondes are similar, the near-surface sampling of the  
307 descending dropsonde are normally made in undisturbed environment away from potential flow

308 distortions such as those near a ship. Hence dropsonde measurements have the potential to  
309 represent the near-surface altitudes better than the ascending rawinsonde carried by balloons.  
310 The hurricane dropsonde dataset provides the best opportunity to assess the application of  
311 dropsonde measurements to EM propagation study and to identify the radar signal ducting  
312 environment in the vicinity of significant tropical disturbances. In this effort, we computed M  
313 from temperature, humidity, and pressure profiles from all available soundings in this data  
314 archive. The vertical gradients of M were used to define different duct layers based on the  
315 criteria outlined in Zhu and Atkinson (2005) and many other references. Figure 8 gives a general  
316 overview of the different duct types occurring in hurricane environment. Here the elevated duct  
317 layers were separated into elevated low ducts (duct heights less than 2 km) and high ducts (duct  
318 heights higher than 2 km). The high level ducts have minimum influence on radar propagation  
319 and communication, but may have an adverse effect on the inversion of GPS radio occultation  
320 data (Ao et al. 2007). Figure 8 shows that ~50% of the soundings show the presence of a duct  
321 layer below 2 km, which is against the general notion that the atmospheric environment in a  
322 hurricane is not in favor of development of ducts. However, Similar result was found by by Ding  
323 et al. (2013) using a much smaller dataset. The ducting layer characteristics were also  
324 categorized in the storm relative environment for the objective of identifying the storm relative  
325 regions critical to radar and communications performance. These characteristics are related to  
326 the cyclone track and other storm related factors using the best track products archived by  
327 NOAA. Statistical analysis methods are used to quantify the characteristics of ducting  
328 conditions in different quadrants of a hurricane relative to its motion. However, no preference of  
329 ducting was identified in any quadrant of the hurricanes. More extensive analyses can be found  
330 in Ziembra (2013).



331 Satellite data play an important role in monitoring and predicting TCs as a result of lack of  
332 in-situ data over the ocean. However, due to the exact same reason, satellite data over the ocean  
333 are not well calibrated and validated. NOAA Products Validation System (NPROVS, Reale et al.  
334 2012) provides a daily compilation and archive of collocated conventional radiosonde (RAOB)  
335 and environmental satellite (SAT) products, which include dropsonde (DROP) observations  
336 routinely available for assimilation into NOAA NCEP GFS forecast models. Wang et al. (2013)  
337 used NPROVS to collocate ten satellite products with the unprecedented dropsonde data  
338 collected during the 2010 Concordiasi field experiment over Antarctica to validate satellite  
339 products. The plan is to compile a dataset containing co-located SAT and DROP temperature and  
340 humidity profiles during 2010-2012 from the QCed dropsondes data from this study. Note that  
341 NPROVS started to operate in 2010. Then we will conduct comparisons of SAT products for  
342 temperature and humidity against DROPS to validate the satellite products in TC environments.  
343 Numerical Weather Prediction products contained in NPROVS can also be evaluated against the  
344 dropsonde data to understand their performance. Additional comparisons against nearby  
345 conventional RAOB can also be included to better understand unique contributions by DROPS  
346 in the context of satellite data validation.

347

#### 348 **4. Conclusions**

349

350 A GPS dropsonde is a scientific instrument deployed from research and operational aircraft,  
351 manned or autonomous, that descends through the atmosphere by a parachute. The GPS  
352 dropsonde was developed in 1995 by NCAR and is currently manufactured by Vaisala, Inc. The  
353 dropsonde provides high-quality, high vertical resolution (~5-15 m) profiles of atmospheric

354 pressure, temperature, relative humidity, wind speed and direction from the aircraft flight level to  
355 the surface over the hard-to-reach areas. Since 1996, GPS dropsondes have been routinely  
356 dropped during hurricane reconnaissance and surveillance flights to help predict hurricane track  
357 and intensity. From 1996 to 2012, NOAA has dropped over 13,000 dropsondes inside hurricane  
358 eye and eyewalls and in the surrounding environment for 120 TCs. All dropsonde data have been  
359 collected, reformatted to one format, and consistently and carefully quality-controlled using  
360 state-of-art QC tools. Three value-added products, the vertical air velocity and the radius and  
361 azimuth angle of each dropsonde location, are generated and added to the dataset. As a result, a  
362 long-term (1996-2012), high-quality, high-vertical resolution GPS dropsonde dataset is created  
363 and made readily available for public access ([https://www.eol.ucar.edu/content/noaa-hurricane-](https://www.eol.ucar.edu/content/noaa-hurricane-dropsonde-archive)  
364 [dropsonde-archive](https://www.eol.ucar.edu/content/noaa-hurricane-dropsonde-archive)). It includes 13,681 quality-controlled dropsonde soundings from 1996 to  
365 2012 for 120 storms.

366 The dropsonde data collected during hurricane reconnaissance and surveillance flights have  
367 significantly improved TC track and intensity forecasts, and enable researchers to better  
368 understand the characteristics of TCs. Previous studies have shown that dropsonde data alone  
369 have improved the hurricane track forecasting by as much as 32% and the hurricane intensity by  
370 20% (Aberson and Franklin 1999). The wind measurements throughout the depth of the  
371 troposphere made by the dropsonde are required to specify the environment flow surrounding the  
372 hurricane eyewall, which determines the hurricane motion (Franklin et al. 2003). The milestones  
373 of dropsonde data's impact on hurricane studies are summarized in the introduction. Various  
374 scientific applications of the long-term dropsonde dataset from this study are highlighted in  
375 Section 3, including characterizing TC structures, studying TC environmental interactions,  
376 identifying surface-based ducts in the hurricane environment which affect electromagnetic wave

377 propagation, and validating satellite temperature and humidity profiling products. We strongly  
378 believe that the applications of this dataset still wait to be discovered by forecasters, researchers  
379 and the general public in the years to come.

380 The extensive and comprehensive QA and QC procedures for dropsonde data are  
381 summarized in this study. They can be applied to other dropsonde data collected over the years.  
382 We plan to find the support to expand our dropsonde dataset in the future by including dropsonde  
383 data from Air Force, NASA, field projects, Taiwan Typhoon surveillance flights and other  
384 countries. From 1997-2012, US Air Force has collected over 6,000 dropsonde profiles. During  
385 last 23 years (1990-2012), the dropsonde system has been deployed to 41 field projects around  
386 the globe and dropped over 8,000 soundings, which includes ones from an unmanned, high-  
387 altitude aircraft (Global Hawk) and stratospheric super-pressure balloons. The Taiwanese  
388 DOSTAR (Dropwindsonde Observations for Typhoon Surveillance near the Taiwan Region)  
389 collected 1,051 soundings from 2003 to 2012 for 49 typhoons (Wu et al. 2005). The inclusion of  
390 these dropsonde data in our archive will further increase the value of the dataset and expand its  
391 applications.

392

393

394 **Acknowledgments:** The dropsonde development over the years is a joint effort of many people  
395 and institutions from national and international community. We thank all who made the  
396 developments and deployments of the dropsonde successful. L. Nguyen is grateful for funding  
397 support from the National Science Foundation grant AGS1132576. Support for P. Black is  
398 gratefully acknowledged through Naval Research Laboratory contract N00173-10-C-6019. The  
399 National Center for Atmospheric Research is sponsored by the National Science Foundation.

400

401 **References:**

402

403 Aberson, S.D., and J. L. Franklin, 1999: Impact on hurricane track and intensity forecasts of  
404 GPS dropwindsonde observations from the first-season flights of the NOAA Gulfstream-IV jet  
405 aircraft. *Bulletin of the American Meteorological Society*, 80(3):421-428, doi:10.1175/1520-  
406 0477.

407 Aberson, S. D., 2010: Ten years of hurricane synoptic surveillance (1997-2006). *Mon. Wea.*  
408 *Rev.*, 138, 1536-1549.

409 Aberson, S. D., 2011: The Impact of dropwindsonde data from the THORPEX Pacific Area  
410 Regional Campaign and the NOAA hurricane field program on tropical cyclone forecasts in the  
411 Global Forecast System. *Mon. Wea. Rev.*, 139, 2689-2703.

412 Ao C. O., 2007: Effect of ducting on radio occultation measurements: an assessment based  
413 on high-resolution radiosonde soundings. *Radio Science*, vol. 42, RS2008,  
414 doi:10.1029/2006RS003485.

415 Barnes, G. M., 2008: Atypical Thermodynamic Profiles in Hurricanes. *Mon. Wea. Rev.*, 136,  
416 631–643.

417 Bean, B. R., and E. J. Dutton, 1966: Radio Meteorology. NBS Monogr., Vol. 92, National  
418 Bureau of Standards, 435 pp.

419 Bell, M. M., and M. T. Montgomery, 2008: Observed structure, evolution, and intensity of  
420 category five Hurricane Isabel (2003) from 12-14 September. *Mon. Wea. Rev.*, 136, 2023-2036.

421 Black, P. G., and coauthors, 2007: Air-sea exchange in hurricanes: Synthesis of observations  
422 from the Coupled Boundary Layer Air-Sea Transfer experiment. *Bull. Amer. Meteor. Soc.*, 88,  
423 357-374.

424 Braun S. A., and W.-K., Tao, 2000: Sensitivity of high-resolution simulations of hurricane  
425 Bob (1991) to planetary boundary layer parameterizations. *Mon. Wea. Rev.*, 128, 3941–3961.

426 Bryan, G. H., and R. Rotunno, 2009: The maximum intensity of tropical cyclones in  
427 axisymmetric numerical model simulations. *Mon. Wea. Rev.*, 137, 1770-1789.

428 Chou, K.-H., C.-C. Wu, P.-H. Lin, S. D. Aberson, M. Weissmann, F. Harnisch, and T.  
429 Nakazawa, 2011: The impact of dropwindsonde observations on typhoon track forecasts in  
430 DOTSTAR and T-PARC. *Mon. Wea. Rev.*, 139, 1728-1743.

431 Corbosiero, K. L., and J. Molinari, 2002: The Effects of Vertical Wind Shear on the  
432 Distribution of Convection in Tropical Cyclones. *Mon. Wea. Rev.*, 130, 2110–2123.

433 DeMaria, M., M. Mainelli, L. K. Shay, J. A. Knaff, and J. Kaplan, 2005: Further  
434 improvements to the Statistical Hurricane Intensity Prediction Scheme (SHIPS). *Wea.*  
435 *Forecasting*, 20, 531–543.

436 Ding, J., J. Fei, X. Huang, and X. Cheng, 2013, Observational occurrence of tropical cyclone  
437 ducts from GPS Dropsonde Data, *J. Appl. Meteor. Climatol.*, 52, 1221–1236.

438 Emanuel, K. A., 1986: An Air-Sea Interaction Theory for Tropical Cyclones. Part I: Steady-  
439 State Maintenance. *J. Atmos. Sci.*, 43, 585-605.

440 Franklin, J. L., M. L. Black, and K. Valde, 2003: GPS dropwindsonde wind profiles in  
441 hurricanes and their operational implications. *Wea. Forecasting*, 18, 32–44.

442 Gopalakrishnan, S. G., F. Marks, J. A. Zhang, X. Zhang, J.-W. Bao and V. Tallapragada,  
443 2013: A study of the impacts of vertical diffusion on the structure and intensity of the tropical  
444 cyclones using the high-resolution HWRF system. *J. Atmos. Sci.*, 70, 524–541.

445 Hamill, Thomas M., Fanglin Yang, Carla Cardinali, Sharanya J. Majumdar, 2013: Impact of  
446 Targeted Winter Storm Reconnaissance Dropwindsonde Data on Midlatitude Numerical Weather  
447 Predictions. *Mon. Wea. Rev.*, 141, 2058–2065. doi: [http://dx.doi.org/10.1175/MWR-D-12-](http://dx.doi.org/10.1175/MWR-D-12-00309.1)  
448 00309.1

449 Hock, T. F., and J. L. Franklin, 1999: The NCAR GPS dropwindsonde. *Bull. Amer. Meteor.*  
450 *Soc.*, 80, 407–420.

451 Molinari, J., D. M. Romps, D. Vollaro, and L. Nguyen, 2012: CAPE in Tropical Cyclones. *J.*  
452 *Atmos. Sci.*, 69, 2452–2463.

453 Molinari, J., J. Frank and D. Vollaro, 2013: Convective Bursts, Downdraft Cooling, and  
454 Boundary Layer Recovery in a Sheared Tropical Storm. *Mon. Weather Rev.*, 141, 1048–1060.

455 Reale T., B. Sun, F. H. Tilley, M. Pettey (2012), The NOAA Products Validation System  
456 (NPROVS), *J. Atmos. Oceanic Technol.*, 29, 629–645. doi: 10.1175/JTECH-D-11-00072.1

457 Riemer, M., M. T. Montgomery, and M. E. Nicholls, 2010: A new paradigm for intensity  
458 modification of tropical cyclones: Thermodynamics impact of vertical wind shear on the inflow  
459 layer. *Atmos. Chem. Phys.*, 10, 3163–3188.

460 Riemer, M., M. T. Montgomery, and M. E. Nicholls, 2013: Further examination of the  
461 thermodynamic modification of the inflow layer of tropical cyclones by vertical wind shear.  
462 *Atmos. Chem. Phys.*, 13, 327–346.

463 Rogers, R. F., and Coauthors, 2013: NOAA'S Hurricane Intensity Forecasting Experiment: A  
464 Progress Report. *Bull. Am. Meteorol. Soc.*, 94, 859–882.

465 Smith, R. K., M. T. Montgomery, and N. Van Sang, 2009: Tropical cyclone spin-up revisited.  
466 *Q. J. Roy. Meteorol. Soc.*, 135, 1321–1335.

467 Szunyogh, I., Z. Toth, R. E. Morss, S. J. Majumdar, B. J. Etherton, and C. H. Bishop, 2000:  
468 The Effect of Targeted Dropsonde Observations during the 1999 Winter Storm Reconnaissance  
469 Program. *Mon. Wea. Rev.*, 128, 3520–3537.

470 Vaisala, 2014: Vaisala Dropsonde RD94. Available on  
471 [http://www.vaisala.com/Vaisala%20Documents/Brochures%20and%20Datasheets/RD94-](http://www.vaisala.com/Vaisala%20Documents/Brochures%20and%20Datasheets/RD94-Dropsonde-Datasheet-B210936EN-A-LoRes.pdf)  
472 [Dropsonde-Datasheet-B210936EN-A-LoRes.pdf](http://www.vaisala.com/Vaisala%20Documents/Brochures%20and%20Datasheets/RD94-Dropsonde-Datasheet-B210936EN-A-LoRes.pdf)

473 Wang, J., J. Bian, W. O. Brown, H. Cole, V. Grubisic, and K. Young, 2009: Vertical air  
474 motion from T-REX radiosonde and dropsonde data. *J. Atmos. Oceanic Technol.*, 26, 928-942.

475 Wang, J., T. Hock, S. A. Cohn, C. Martin, N. Potts, T. Reale, B. Sun and F. Tilley, 2013:  
476 Unprecedented upper air dropsonde observations over Antarctica from the 2010 Concordiasi  
477 Experiment: Validation of satellite-retrieved temperature profiles. *Geophys. Res. Lett.*, DOI:  
478 10.1002/grl.50246.

479 Weissmann, M., F. Harnisch, C.-C. Wu, P.-H. Lin, Y. Ohta, K. Yamashita, Y.-H. Kim, E-H.  
480 Jeon, T. Nakazawa, and S.D. Aberson. The influence of assimilating dropsonde data on typhoon  
481 track and mid-latitude forecasts. *Monthly Weather Review*, 139(3):908-920,  
482 doi:10.1175/2010MWR3377.1

483 Wu, C.-C., P.-H. Lin, S. Aberson, T.-C. Yeh, W.-P. Huang, K.-H. Chou, J.-S. Hong, G.-C.  
484 Lu, C.-T. Fong, K.-C. Hsu, I-I Lin, P.-L. Lin, C.-H. Liu, 2005: Dropsonde Observations for

485 Typhoon Surveillance near the Taiwan Region (DOTSTAR): An overview. *Bulletin of Amer.*  
486 *Meteor. Soc.*, **86**, 787-790.

487 Wu, C.-C., K.-H. Chou, P.-H. Lin, S. D. Aberson, M. S. Peng, and T. Nakazawa, 2007: The  
488 impact of dropwindsonde data on typhoon track forecasts in DOTSTAR. *Weather and*  
489 *Forecasting*, 22, 1157-1176.

490 Wu, C.-C., S.-G. Chen, C.-C. Yang, P.-H. Lin, and S. D. Aberson, 2012: Potential vorticity  
491 diagnosis of the factors affecting the track of Typhoon Sinlaku (2008) and the impact from  
492 dropwindsonde data during T-PARC. *Mon. Wea. Rev.*, 140, 2670-2688.

493 Zhang, J. A., R. F. Rogers, P. D. Reasor, E. W. Uhlhorn, and F. D. Marks, 2013: Asymmetric  
494 Hurricane Boundary Layer Structure from Dropsonde Composites in Relation to the  
495 Environmental Vertical Wind Shear. *Mon. Wea. Rev.*, 141, 3968–3984.

496 Zhang, J. A., 2010: Estimation of dissipative heating using low-level in-situ aircraft  
497 observations in the hurricane boundary layer. *J. Atmos. Sci.*, 67, 1853-1862.

498 Zhang, J. A., P. G. Black, J. R. French, and W. M. Drennan, 2008: First direct measurements  
499 of enthalpy flux in the hurricane boundary layer: the CBLAST results. *Geophys. Res. Lett.*,  
500 35(11): L14813, doi:10.1029/2008GL034374.

501 Zhang, J. A., R. F. Rogers, D. S. Nolan, and F. D. Marks, Jr., 2011: On the characteristic  
502 height scales of the hurricane boundary layer. *Mon. Weather Rev.*, 139, 2523-2535.

503 Zhang, J.A., R.F. Rogers, P. Reasor, E.W. Uhlhorn, and F.D. Marks, 2013: Asymmetric  
504 hurricane boundary layer structure from dropsonde composites in relation to the environmental  
505 vertical wind shear. *Mon. Weather Rev.*, 141, 3968-3984.

506 Zhu, M. and B. W. Atkinson, 2005: Simulated Climatology of Atmospheric Ducts over the  
507 Persian Gulf. *Boundary Layer Meteorol.* 115(3), pp. 433-452.



508        Ziemba, D. A., 2013: Ducting conditions for electromagnetic wave propagation in tropical  
509        disturbances from GPS dropsonde data. M. S. Thesis, Naval Postgraduate School.  
510  
511

512 **Table and Figure captions:**

513

514 Table 1. The list of major milestones in AVAPS advancement and scientific impact during 1995-  
515 2012.

516 Fig. 1 Improvement of mean hurricane track forecast in the GFS model as a result of assimilating  
517 synoptic surveillance dropsondes during 1999-2005. Number of forecasts is also given.

518 Fig. 2 Numbers of soundings (black line) and storms in each year from 1996 to 2012 included in  
519 the final dataset.

520 Fig. 3 Maps of dropsonde locations from NOAA G-IV (black dots) and P3 (red dots) for each  
521 year. Total number of soundings for each year is given in the legend.

522 Fig. 4 Dropsonde locations from NOAA P3 (magenta balloons) and NOAA G-IV (green  
523 balloons) between 17 UTC and 24 UTC on August 28, 2005 for Hurricane Katrina. The blue line  
524 is the hurricane track. The background color image shows the satellite water vapor image.

525 Fig. 5 (a) Number of dropsondes in each 100-km radial bin. (b) Number of dropsondes in each  
526 30° azimuthal bin. The azimuthal direction follows meteorological convention (i.e. 90° denotes  
527 a dropsonde that is east of the tropical cyclone center).

528 Fig. 6 Mean wind speed profiles for Hurricane category 1-5 computed from 3,101 dropsonde  
529 profiles. The number of soundings used for each category is given in the legend.

530 Fig. 7 (a) Mean equivalent potential temperature of the 75-200 km radii region in the  
531 downshear-left (DSL; solid red), downshear-right (DSR; dashed orange), upshear-left (USL;  
532 dotted blue), and upshear-right (USR; dash-dotted blue) quadrants in tropical cyclones embedded  
533 in greater than 6 m s<sup>-1</sup> of ambient vertical wind shear. (b) Number of data points at each vertical  
534 level in each quadrant.

535 Fig. 8 Frequency occurrences of various duct types in hurricane environment from all hurricanes  
536 with dropsonde measurements as well as storm track data. The numbers in parentheses denote  
537 the number of dropsondes with the specific duct type. The 'elevated lower' category refers to  
538 elevated ducts below 2 km. The 'elevated high' category refers to a single elevated duct layer  
539 above 2 km.

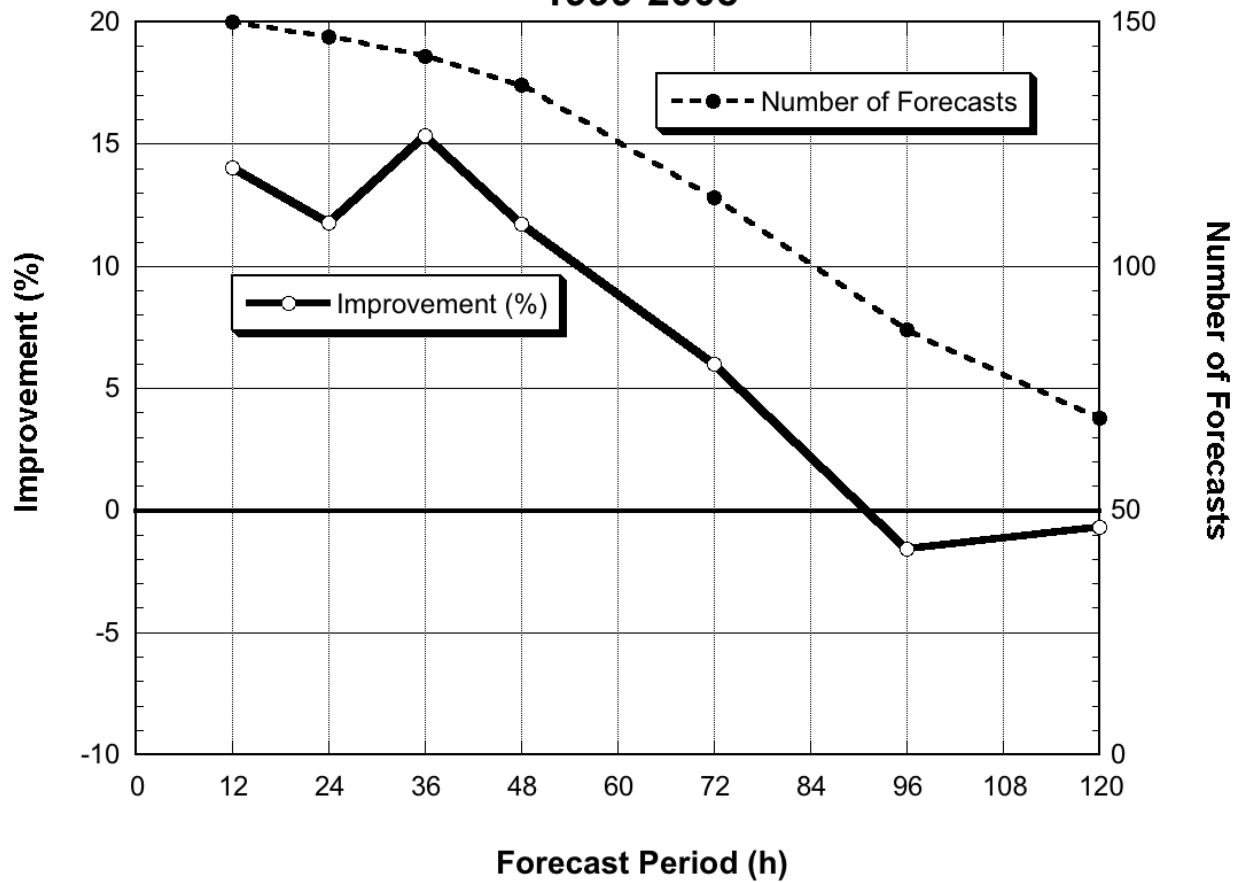
540

541

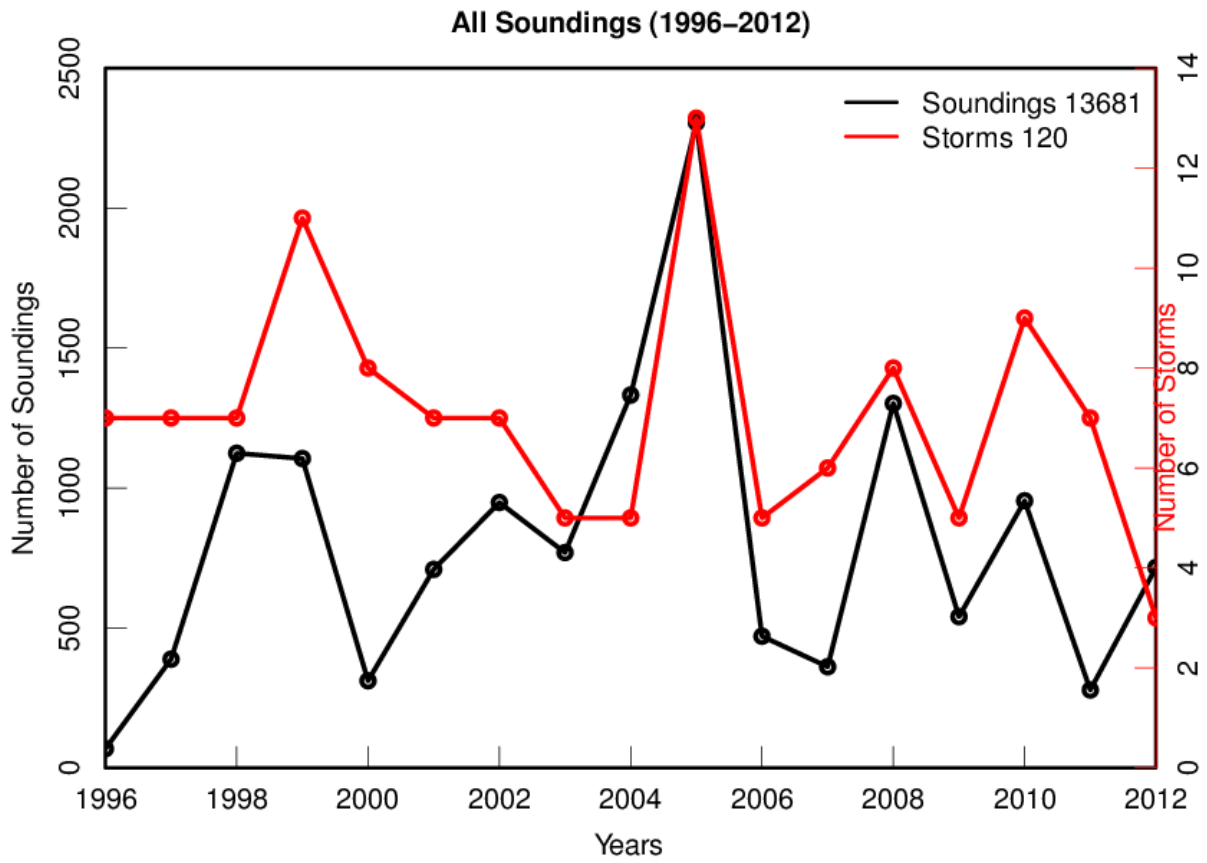
542 Table 1. The list of major milestones in AVAPS advancement and scientific impact during 1995-  
 543 2012.  
 544

Years	Milestones	Impact
1995	<ul style="list-style-type: none"> <li>• The world-first GPS dropsonde system (referred as to AVAPS) was under development at NCAR.</li> <li>• Dropsonde uses Vaisala PTH module RSS903 and GPS codeless receiver GPS-111/121 for winds.</li> <li>• A single version software supported up to four simultaneous dropsonde soundings, the first for atmospheric sounding systems, and operations on many different aircraft platforms.</li> </ul>	<ul style="list-style-type: none"> <li>• The GPS dropsonde development made it possible to obtain vertical profiles of wind and thermodynamic parameters within nearly all portions of the hurricane with unprecedented accuracy and resolution.</li> <li>• The ~150 sondes from the first G-IV mission resulted in a 30% improvement in 24-36-h hurricane track forecasts (Aberson and Franklin 1999).</li> </ul>
1996	<ul style="list-style-type: none"> <li>• The AVAPS development was completed.</li> <li>• First deployment of system on NOAA G-IV for test flights.</li> <li>• NCAR Licenses AVAPS technology to Vaisala Inc.</li> </ul>	
1997	<ul style="list-style-type: none"> <li>• First supported field campaign for FASTEX (Fronts and Atlantic Storm Track Experiment), which used over 800 dropsondes released from three different aircraft.</li> <li>• NOAA began operational hurricane missions with the AVAPS on both G-IV and P3.</li> </ul>	<ul style="list-style-type: none"> <li>• The first deployment of GPS sondes in the eyewall of Hurricane Guillermo on 2-4 August 1997 illustrated the complex variability of boundary layer structure in the hurricane (Hock and Franklin 1999).</li> </ul>
2005	<ul style="list-style-type: none"> <li>• GPS receiver is changed to u-blox TIM-LF receiver (from GPS-121) to increase wind solution from 2Hz to 4Hz and improve its reliability.</li> </ul>	<ul style="list-style-type: none"> <li>• The usage of u-blox GPS receiver increases the wind sampling from 2Hz to 4Hz to detect more detailed structure and make the last wind data point closer to the ocean surface.</li> </ul>
2006	<ul style="list-style-type: none"> <li>• GPS receiver is changed to u-blox TIM-4P from TIM-LF to improve its reliability.</li> </ul>	
2008	<ul style="list-style-type: none"> <li>• Major redesign of AVAPS system, and it is renamed as “AVAPS II”.</li> <li>• Improvement includes u-blox TIM-5P GPS receiver for winds, Vaisala RSS904 module for PTH, a more robust telemetry system resulted in higher percentage of GPS data per sounding, latest technology for electronics and firmware, reduction in mass of dropsonde, ability for eight simultaneous soundings.</li> <li>• AVAPS II software user interface retained the same basic look and feel to the dropsonde operator, thus minimizing the trouble and expense of retraining experienced flight crews.</li> </ul>	<ul style="list-style-type: none"> <li>• AVAPS II significantly reduces the percentage of the GPS wind loss (two third) and the time to obtain the winds in the beginning from ~30s to ~1s.</li> <li>• The capability of 8 simultaneous soundings makes it possible to sample the atmosphere in much higher horizontal spatial resolution.</li> </ul>
2010	<ul style="list-style-type: none"> <li>• Significant internal enhancement of the software to allow remotely controlled operation via satellite communications link for use on the unmanned NASA Global Hawk aircraft and super pressure balloons (driftsonde system).</li> <li>• Development of Mini Dropsonde with smaller size and lighter weight for NASA Global Hawk and a fully automated remote control aircraft system. a slightly different version of this sonde is also used for Driftsonde</li> </ul>	<ul style="list-style-type: none"> <li>• The development of mini dropsonde, completely automatic operations and new platforms extend the dropsonde’s vertical dimension to the UT/LS regions, lengthen its deployment duration and increase its spatial coverage, and thus expand to new scientific areas.</li> </ul>

### Impact of Synoptic Surveillance Dropwindsondes on GFS Track Forecasts 1999-2005

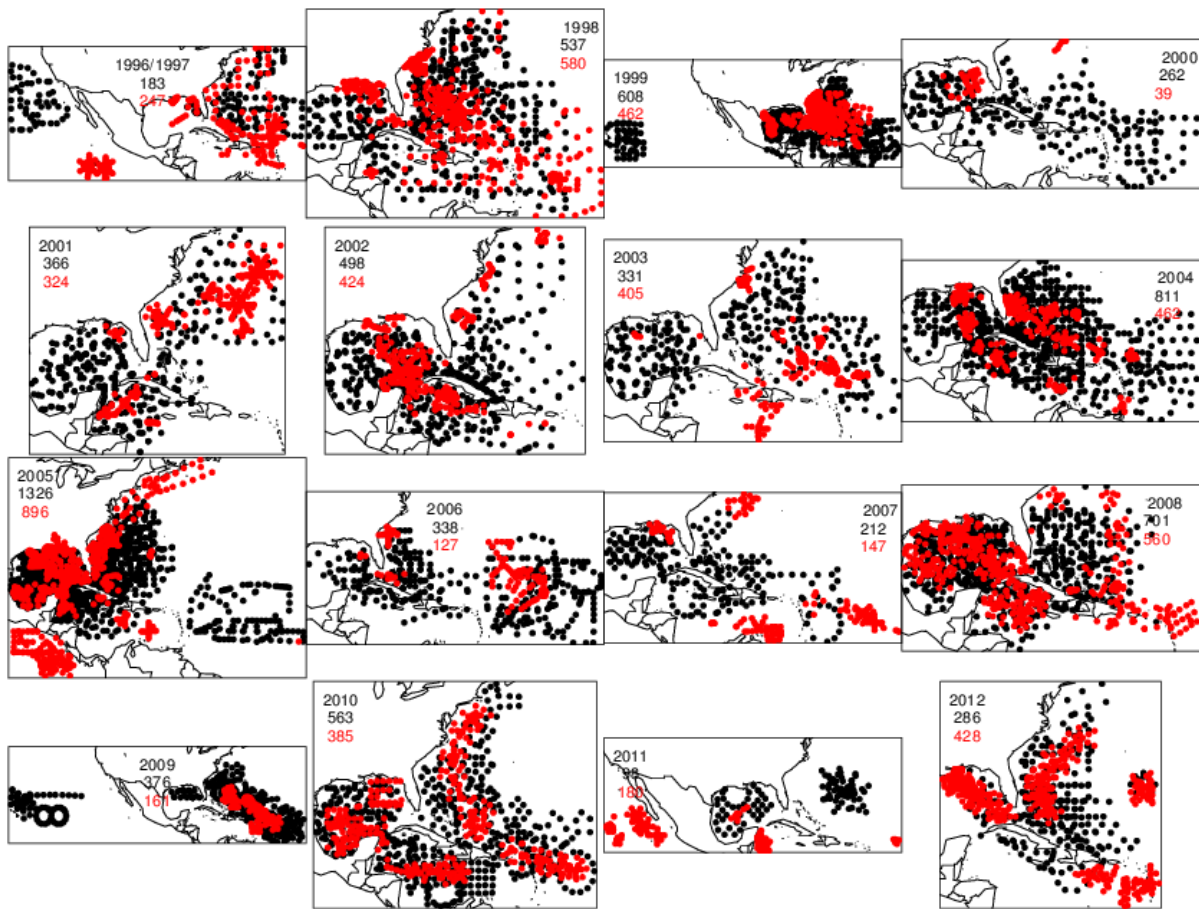


545  
 546  
 547 Fig. 1 Improvement of mean hurricane track forecast in the GFS model as a result of assimilating  
 548 synoptic surveillance dropsondes during 1999-2005. Number of forecasts is also given.



549

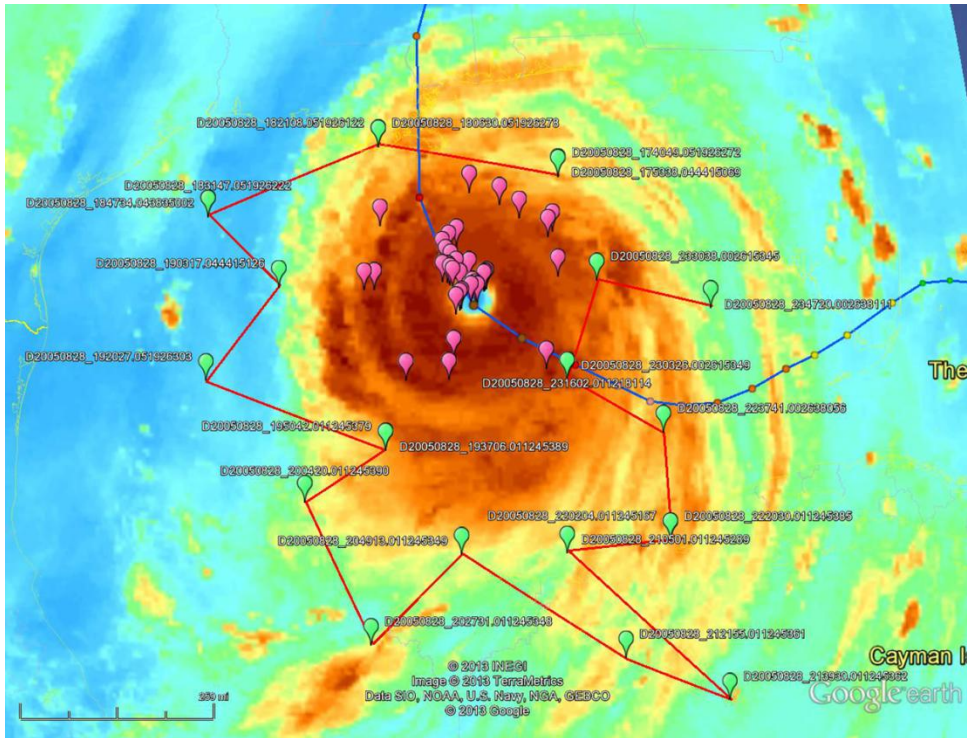
550 Fig. 2 Numbers of soundings (black line) and storms in each year from 1996 to 2012 included in  
 551 the final dataset.



552

553 Fig. 3 Maps of dropsonde locations from NOAA G-IV (black dots) and P3 (red dots) for each  
 554 year. Total number of soundings for each year is given in the legend.

555



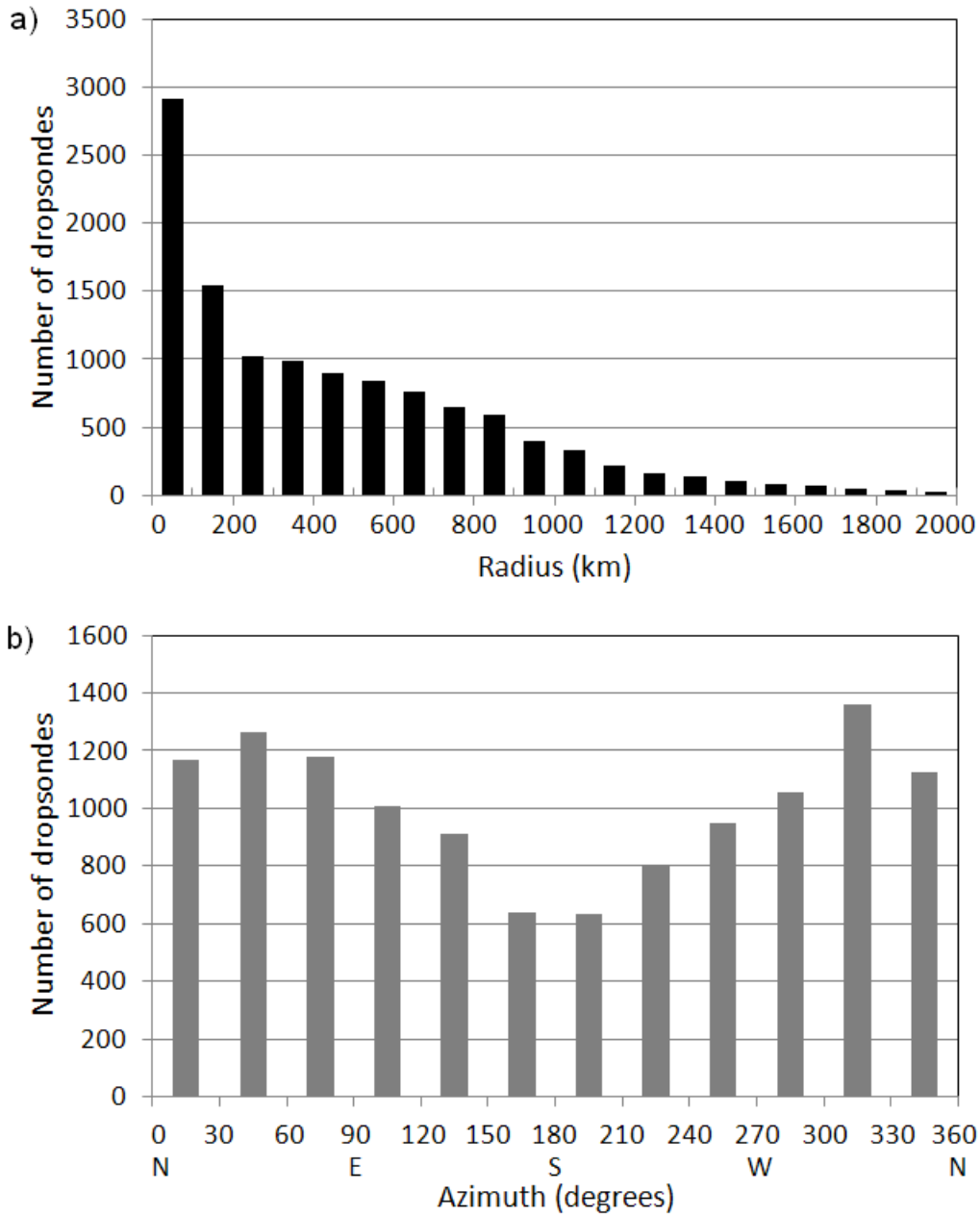
556

557 Fig. 4 Dropsonde locations from NOAA P3 (magenta balloons) and NOAA G-IV (green  
 558 balloons) between 17 UTC and 24 UTC on August 28, 2005 for Hurricane Katrina. The blue line  
 559 is the hurricane track. The background color image shows the satellite water vapor image.

560

561

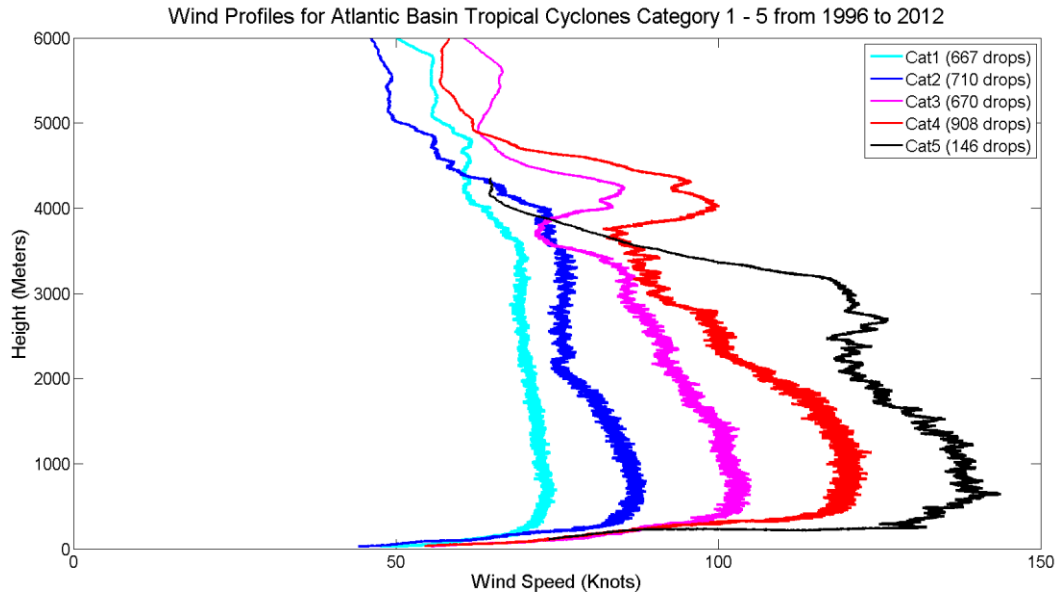




562

563 Fig. 5 (a) Number of dropsondes in each 100-km radial bin. (b) Number of dropsondes in each  
 564 30° azimuthal bin. The azimuthal direction follows meteorological convention (i.e. 90° denotes  
 565 a dropsonde that is east of the tropical cyclone center).

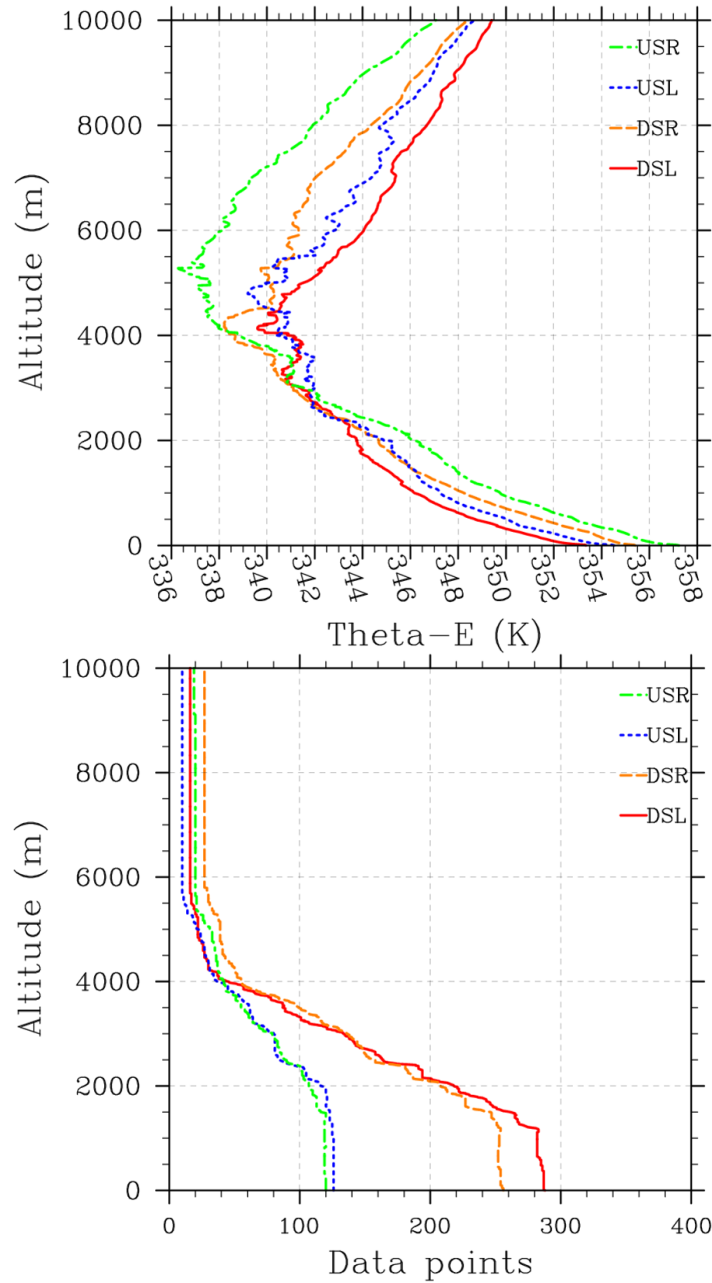
566



567

568 Fig. 6 Mean wind speed profiles for Hurricane category 1-5 computed from 3,101 dropsonde  
 569 profiles. The number of soundings used for each category is given in the legend.

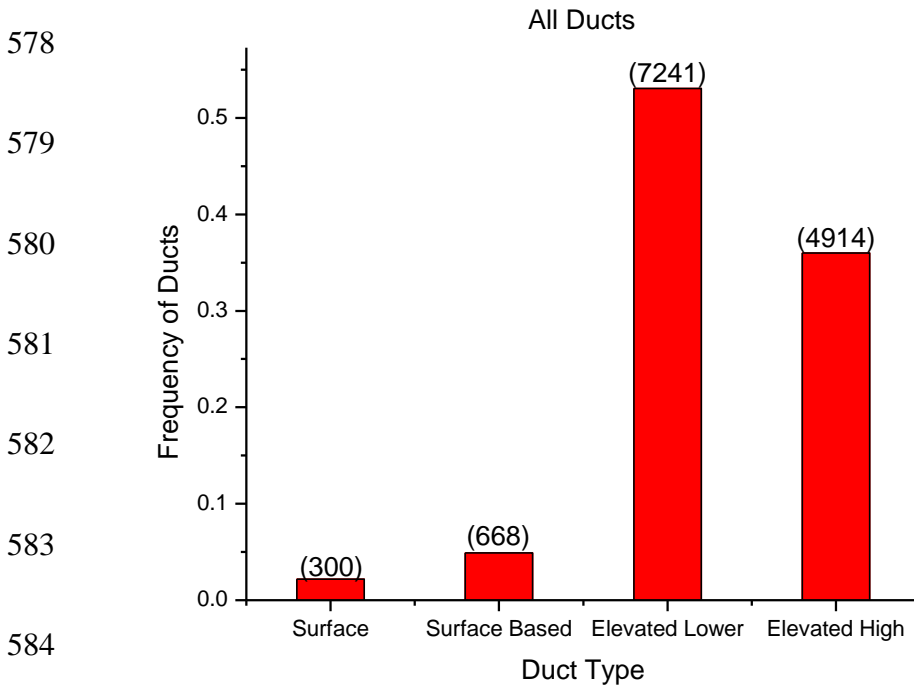
570



571

572

573 Fig. 7 (upper panel) Mean equivalent potential temperature of the 75-200 km radii region in the  
 574 downshear-left (DSL; solid red), downshear-right (DSR; dashed orange), upshear-left (USL;  
 575 dotted blue), and upshear-right (USR; dash-dotted blue) quadrants in tropical cyclones embedded  
 576 in greater than 6 m s<sup>-1</sup> of ambient vertical wind shear. (lower panel) Number of data points at  
 577 each vertical level in each quadrant.



585 Fig. 8 Frequency occurrences of various duct types in hurricane environment from all hurricanes  
 586 with dropsonde measurements as well as storm track data. The numbers in parentheses denote  
 587 the number of dropsondes with the specific duct type. The 'elevated lower' category refers to  
 588 elevated ducts below 2 km. The 'elevated high' category refers to a single elevated duct layer  
 589 above 2 km.